

ACCEPTED MANUSCRIPT

Abstract

Stress hormones have been shown to be important mediators in driving malignant growth and reducing treatment efficacy in breast cancer. Glucocorticoids can induce DNA damage through an inducible nitric oxide synthase (iNOS) mediated pathway to increase levels of nitric oxide (NO). Using an immune competent mouse breast cancer model and 66CL4 breast cancer cells we identified a novel role of NOS inhibition to reduce stress-induced breast cancer metastasis. On a mechanistic level we show that the glucocorticoid cortisol induces expression of key genes associated with angiogenesis, as well as pro-tumourigenic immunomodulation. Transcriptomics analysis confirmed that in the lungs of tumour-bearing mice, stress significantly enriched pathways associated with tumourigenesis, some of which could be regulated with NOS inhibition. These results demonstrate the detrimental involvement of NOS in stress hormone signalling, and the potential future benefits of NOS inhibition in highly stressed patients.

1 **Stress hormone-mediated acceleration of breast cancer metastasis is halted by inhibition of nitric**
2 **oxide synthase.**

3

4 Renée L. Flaherty*, Haya Intabli*, Marta Falcinelli*, Giselda Bucca*, Andrew Hesketh*, Bhavik A.
5 Patel*, Marcus C. Allen*, Colin P. Smith*, Melanie S. Flint*+

6 *School of Pharmacy and Biomolecular Sciences, University of Brighton, Moulsecoomb, Brighton,
7 BN2 4GJ, UK

8 Centre for Stress and Age-related Disease.

9 +corresponding author

10

11 **Abstract**

12 Stress hormones have been shown to be important mediators in driving malignant growth and
13 reducing treatment efficacy in breast cancer. Glucocorticoids can induce DNA damage through an
14 inducible nitric oxide synthase (iNOS) mediated pathway to increase levels of nitric oxide (NO). Using
15 an immune competent mouse breast cancer model and 66CL4 breast cancer cells we identified a
16 novel role of NOS inhibition to reduce stress-induced breast cancer metastasis. On a mechanistic
17 level we show that the glucocorticoid, cortisol induces expression of keys genes associated with
18 angiogenesis, as well as pro-tumourigenic immunomodulation. Transcriptomics analysis confirmed
19 that in the lungs of tumour-bearing mice, stress significantly enriched pathways associated with
20 tumourigenesis, some of which could be regulated with NOS inhibition. These results demonstrate
21 the detrimental involvement of NOS in stress hormone signalling, and the potential future benefits
22 of NOS inhibition in highly stressed patients.

23 **Keywords**

24 Breast cancer; Glucocorticoids; Stress

25

26

27

28

29

30

31

32 1. Introduction

33 Psychological stress induces an increase in the circulating levels of stress hormones, including the
34 glucocorticoid cortisol. [1]. Epidemiological evidence has associated negative psychosocial factors,
35 including chronic stress, with increased incidence and poorer survival in breast cancer patients [2].
36 Furthermore, multiple studies have linked psychological stress with biological processes involved in
37 metastasis [3-5], findings of particular importance since the primary cause of breast cancer-related
38 death is metastatic spread [6].

39 Glucocorticoid signalling, mediated through the glucocorticoid receptor (GR), has been shown to
40 promote tumorigenesis and drug-resistance in triple negative breast cancer (TNBC) [7], and
41 increases in expression of GR in breast tumours have been correlated with decreased survival [8]. GR
42 antagonism has also previously been shown to induce apoptosis and, in combination with
43 conventional chemotherapies, reduce tumour size in models of TNBC [9]. We have previously
44 explored the mechanistic actions of psychological stress in breast cancer, and shown that stress
45 hormone exposure can induce DNA damage in breast cancer through the generation of reactive
46 oxygen and nitrogen species (ROS/RNS). We have also previously shown that glucocorticoids
47 mediate a non-genomic effect on inducible nitric oxide synthase (iNOS), the enzyme that generates
48 NO, and increase nitric oxide (NO) signalling in breast cancer cells [10]. Although iNOS is expressed in
49 both ER+ and ER- breast cancers [11, 12], expression of iNOS has been found to correlate with
50 tumour progression and poor survival in basal-like breast cancers [13, 14], indicating that NO activity
51 may drive malignant growth and spread. As such, iNOS represents a potential target to abrogate the
52 detrimental effects of psychological stress hormone signalling.

53 Nitric oxide (NO) is an important signalling molecule modulating a range of functions within the cell,
54 however the role of NO in tumour biology is complex and multifaceted [15]. Aspects of tumourigenic
55 transformation can be driven by prolonged inflammation and exposure to high concentrations of
56 NO, resulting in an increase in oxidative stress and subsequent DNA damage [16]. It is thought that
57 NO may also be capable of driving transformation through the induction of angiogenesis and
58 migration [17]. The highest concentrations of NO are produced by iNOS, and expression of iNOS has
59 been shown to be positively correlated with tumour grade, stage and metastasis in breast cancer
60 [11, 18-20]. Several studies have shown that induction of iNOS expression in tumour cells promotes
61 an increase in angiogenesis, and subsequently an increase in invasiveness and progression [16] [21,
62 22]. However transfection of iNOS in certain tumour types has been proven to inhibit growth, and
63 when delivered as a gene therapy extends survival of metastases-bearing mice [23]. The biphasic

64 effect of NO is therefore dependent on localization, expression and activity of NOS isoforms as well
65 as the concentration and length of exposure to NO.

66 Selective or non-selective inhibition of NOS as a potential therapy has been studied in relation to
67 cancer, and has been shown to decrease angiogenesis, tumour growth and metastases and increase
68 survival in breast cancers [14, 16, 22, 24-26]. As such, our aim is to determine whether non-selective
69 inhibition of NOS in the context of highly metastatic mammary tumours may abrogate the NO-
70 mediated metastatic signalling induced by psychological stress.

71 **2. Methods**

72 2.1 Cells and Culture Conditions

73 The murine cell line 66CL4 (RRID:CVCL_9721), derived from a spontaneously-arising mammary
74 tumour, were kindly donated by Dr Erica Sloan; Monash University Australia and maintained in MEM
75 with 10% FBS (Gibco, UK). Human breast cancer cell line MCF-7 (RRID:CVCL_0031) was purchased
76 from ATCC and maintained in Dulbecco's Modified Eagle Medium (DMEM) (Gibco, UK) with 10% FBS
77 (Gibco, UK). MCF-7 cells were chosen as a comparator as they express similar levels of GR expression
78 compared to human triple negative breast cancer (TNBC) cell lines [27] and also are known to
79 express iNOS [12]. All cell lines were maintained in humid conditions at 37°C and with 5%
80 atmospheric CO₂. Cells were treated with hydrocortisone (Sigma Aldrich, UK) at a concentration of
81 5µM, and all other pharmacological agents as stated previously [10].

82 2.2 Electrochemistry

83 Electrodes were fabricated by modification of a previously published approach [28]. Characterisation
84 was carried out as detailed previously [10]. 66CL4 and MCF-7 cells were plated at a density of 5x10⁴
85 per well and incubated for 24 hrs. Cells were exposed to cortisol in the presence and absence of
86 RU486, 1400W dihydrochloride or L-NAME for 30mins prior to hormone treatment. Cells were
87 immediately lysed and ROS/RNS levels were quantified using multiple-step amperometry using a
88 stainless steel counter electrode and non-leak Ag|AgCl reference electrode. Measurements of the
89 current were obtained at +0.3 V, +0.45 V, +0.62 V and +0.85 V for a duration of 30 s. The responses
90 were analysed using approaches detailed in [29], using a CHI760E potentiostat (CH Instruments,
91 Texas, USA).

92 2.3 Griess Assay

93 66CL4 and MCF-7 cells were plated at a density of 3x10⁵ per well of a 6 well plate. Cells were treated
94 with cortisol in the presence or absence of RU486 or L-NAME for 30mins. Cell culture media was

95 removed and assayed for extracellular nitrite using the Griess Reagent System (Promega, UK), as per
96 the manufacturer's instructions.

97 2.4 Immunofluorescence

98 Cells plated on glass coverslips and treated. Cells were then fixed in 3% paraformaldehyde 2%
99 sucrose (pH 7.2) PBS for 10 minutes, washed, and permeabilized using 0.2% TritonX-100 in PBS for
100 2.5mins at room temperature. Incubation with the primary antibody; anti-phospho-Histone H2AX
101 (1:800 in 2% BSA) (Cell Signalling, RRID:AB_2118010), anti-RAD51 (1:200 in 2% BSA) (Cell Signalling,
102 RRID:AB_2721109) or anti-GR (1:200 in 2% BSA) (Santa Cruz Biotech, RRID:AB_2155786) occurred for
103 45 mins at 37°C and the secondary antibody; anti-rabbit IgG FITC (1:200 in 2% BSA) (Sigma Aldrich,
104 RRID:AB_259682) at 37°C for 20 mins. Fluorescent foci were detected using confocal microscopy
105 (Leica, Germany) and positive cells, categorised as >5 foci, expressed as a percentage of total cells
106 counted.

107 2.5 In Vivo Study

108 All *in vivo* studies were carried out with Home Office approval and approved by the Animal Welfare
109 and Ethical Review Body (AWERB) at the University of Brighton. All animal experiments comply with
110 the ARRIVE guidelines and were carried out in accordance with the U.K. Animals (Scientific
111 Procedures) Act, 1986 Female BALB/c mice were purchased at 6 weeks old from Envigo. They were
112 housed 5 per cage with food and water *ad libitum* in a 12 hour light/dark cycle. Mice were handled
113 daily for 1 week prior to experimentation to acclimatise the mice to the investigator. Tumours were
114 induced by the subcutaneous injection of 1×10^5 66CL4 cells were injected into the 4th mammary fat
115 pad. Tumours were measured using digital callipers until they reached 150-200mm³, mice were then
116 randomized into groups (n=9). Groups were treated with intraperitoneal (IP) injections of saline or L-
117 NAME (80mg/kg dissolved in saline) (Sigma Aldrich, UK). To induce psychological stress a restraint
118 stress model previously described [30] was used. Mice were individually placed in adequately
119 ventilated 50ml conical tubes for 2hrs 6 days a week for 2 weeks. Tumour volumes were measured
120 twice a week using digital callipers and calculated using the formula for an ellipsoid sphere; volume
121 (mm³) = shortest (S)² x longest (L) x 0.52. Mice were also weighed once a week. Mice were sacrificed
122 after 2 weeks of treatment. Animals that were sacrificed before the endpoint of the study due to
123 tumour burden were excluded from the study. Primary tumours were weighed, dissected and cut in
124 half, with half flash frozen in liquid nitrogen and half fixed in 10% neutral buffered formalin. Lungs
125 were also removed, one half (lobe) was fixed in formalin and the other flash frozen in liquid
126 nitrogen.

127 2. 6 Bone Marrow-Derived Macrophage Isolation and Culture

128 Female BALB/c 6-8weeks old were sacrificed and primary bone marrow-derived macrophages
129 (BMDM) were isolated from the femurs and tibiae as described in [31]. BMDM's were cultured in
130 RPMI-1640 with 10% FBS, 100 U/ml penicillin, 100 µg/ml streptomycin (Gibco, UK) and
131 supplemented with 10ng/ml M-CSF (Peprotech, UK). Growth media was changed on day 3, and on
132 day 7 M-CSF was removed and BMDM were polarized to M1 by the addition of 100ng/ml LPS (Sigma
133 Aldrich, UK), or M2 by the addition of 10ng/ml IL-4 (Peprotech, UK). Polarization was confirmed
134 using qPCR to determine the expression of iNOS, arginase 1 (Arg1) and CCR2.

135 2. 7 3D Spheroid Co-culture

136 66CL4 cells and polarized BMDM's were collected by scraping and 1×10^6 cells resuspended in 1ml of
137 serum free media. The lipophilic tracer dyes SP-DiOC₁₈(3) (66CL4) or DiI (BMDM) (Thermo Fisher,
138 UK) were added at a concentration of 5µg/ml and the cells incubated at 37°C for 1hr. Cells were
139 washed with PBS and combined in a ratio of 2000:1000 66CL4 to BMDM, or 2000 66CL4 cells alone
140 in 30µl/well of a 96-well Ultra Low Attachment plate (Corning, UK). The plates were centrifuged at
141 300g for 5mins and incubated at 37°C and with 5% atmospheric CO₂ for 7 days. Each day media was
142 removed and the spheroids treated with fresh media alone, cortisol 5µM, L-NAME 100µM or a
143 combination of cortisol and L-NAME.

144 2. 8 ELISA

145 The levels of CCL2 and IL-10 in the media from co-cultured 66CL4/BMDM spheroids was measured
146 using a CCL2 or IL-10 ABTS ELISA kit (Peprotech, UK) as per the manufacturers instructions. Levels
147 were normalized to protein extracted from the spheroids (mg/mL).

148 2. 9 Immunohistochemistry

149 Formalin fixed tissues were processed using standard histological practices (Leica TP1050) and
150 embedded into paraffin wax. For CD31 staining - Sections were dewaxed and subsequently
151 transferred to antigen retrieval buffer (Tris/ EDTA/ Tween-20) at 95°C for 20 minutes.
152 Permeabilization (0.1% Triton-X in PBS) and blocking (2% BSA in PBs) followed. Sections were
153 incubated with the primary antibody anti-CD31 (Abcam, RRID:AB_726362) and secondary anti-rabbit
154 FITC conjugated (Sigma Aldrich, UK) for 1 hour and 30 minutes at room temperature respectively.
155 Areas of high microvessel density were identified at low magnification (x20), and at (x63) the
156 number of small CD31-positive vessels were counted per field.

157 For KI67 staining - staining was performed Using Benchmark ULTRA autostainer (Ventana Medical
158 Systems) as per the standard protocol. Slides were imaged at x20 magnification using GXcapture
159 software and KI67 labelling index analysed using ImmunoRatio [32]. Sections of fixed lungs were also
160 taken through the midline and stained with Haematoxylin and eosin (H&E). Metastatic nodules were
161 histologically identified at low magnification (x10) and counter per lung section.

162 2. 10 qPCR

163 66CL4 cells were treated with cortisol for 30mins and 24hrs. RNA was extracted from cells and tissue
164 using an RNeasy Kit (Qiagen, UK) and cDNA was synthesised using a Quantitect Reverse Transcription
165 kit (Qiagen, UK) as per the manufacturer's instructions. A Rotor-Gene SYBR Green (Qiagen, UK)
166 master mix was prepared according to the manufacturer's instructions using Quantitect Primer
167 Assay for mouse *ACTB*, *NOS2*, *VEGFA*, *TWIST1*, *CCL2* and *ARG1* (Qiagen, UK). Ct values were obtained
168 using Rotor-Gene Q software. Change in expression was measured using the $\Delta\Delta C_t$ method and
169 expressed as relative expression versus the experimental control or an internal universal reference.

170 2. 11 Western Blot

171 Cells were lysed in ice cold radioimmunoprecipitation assay (RIPA) buffer (150 mM NaCl, 1% 10
172 NP40/Igepal, 0.5% NaDoC, 0.1% SDS, 50 mM protease inhibitor (Sigma Aldrich, UK)) for 1–2 minutes.
173 The lysates were subsequently spun at 13,000 g for 14 minutes at 4 °C. Protein concentration was
174 determined using a DC protein assay (BioRad, UK) and 10 μ g resolved on SDS-PAGE gels (10%
175 resolving and 4.5% stacking) and transferred onto polyvinylidene fluoride (PVDF) membranes.
176 Membranes were blocked in 5% BSA (Sigma Aldrich, UK) and incubated with the following primary
177 antibodies; iNOS 1:2000 in 5% BSA (Santa Cruz, RRID:AB_2298577) and β -actin 1:10000 (Santa Cruz,
178 RRID:AB_2714189) overnight at 4 °C, and appropriate secondary antibodies (Anti-rabbit/mouse IgG-
179 HRP, Santa Cruz, RRID:AB_631746/ RRID:AB_10915700) 1:2000 in 2.5% BSA for 1 h at room
180 temperature. The membranes were developed using Amersham ECL Prime detection kit and
181 exposed to Amersham Hyperfilm. The film was then processed using a developing system (Xograph
182 Compact X4) and imaged in a Chemi Imager (Alpha Inotech).

183 2. 12 Migration assay

184 66CL4 cells were transfected with *NOS2*-directed siRNA alongside a scrambled control (100 μ M)
185 (Qiagen, UK) using lipofectamine 2000 (10 μ g/ml) (Fisher, UK) in Opti-MEM media (Gibco, UK). Cells
186 were incubated overnight and replated at a density of 6x10⁵ cells/well in MEM containing no FBS
187 with or without cortisol (5 μ M) onto transwell inserts (8 μ M pores). The lower chamber was filled
188 with MEM+10% FBS and the cells incubated for 4 hours. After 4 hours inserts were removed, and

189 cells that did not migrate on the top of the membrane were removed using a cotton swab. Cells on
190 the underside were fixed with 3% PFA, stained with Mayer's Haematoxylin and counted (x20). Data
191 is expressed as cells per field.

192 2. 13 Scratch Assay

193 66CL4 cells were plated at a density of 1×10^5 in a 12 well plate and grown to confluency. A 'scratch'
194 was made using a p200 pipette tip and the cells treated with antagonists (RU486, L-NAME or 1400W)
195 for 30mins prior to the addition of cortisol. Images were taken at 0hrs and 24hrs. Area of the wound
196 was measured using ImageJ and expressed as area closure relative to the 0hr time point.

197 2. 14 Cell Viability Assay

198 66CL4 cells were plated at a density of 1×10^4 cells/well in a 96 well plate. Cells were treated with
199 treated with antagonists (RU486, L-NAME or 1400W) for 30mins prior to the addition of cortisol and
200 incubated for 48hrs. Cell viability was determined by incubating the cells with 0.2mg/ml MTT
201 powder dissolved in cell culture media. Plates were protected from the light and incubated for 2hrs
202 at 37°C. The MTT solution was removed and replaced with 200µL dimethyl sulfoxide (DMSO), the
203 plate shaken for 5mins and absorbance read at 495nm (Digiread). Cell viability is expressed as a
204 percentage of the control.

205 2. 15 Transcriptomics

206 Total RNA was extracted from whole lungs flash frozen in liquid nitrogen immediately after removal
207 from sacrificed animals. Lung tissues were immersed in RNA-later ice solution over night at 4°C
208 (Thermo Fisher Scientific, UK) to stabilize the mRNA populations prior to tissue homogenization.
209 Lung tissues were homogenized in a Tissue Lyser (Qiagen, UK) 2x 2 min at 30 rpm and centrifuged at
210 13.2K rpm for 3 min to remove cell debris. Total RNA was extracted using RNeasy mini columns
211 (Qiagen, UK) with an additional step of genomic DNA removal through agDNA eliminator column.

212 RNA was quantified using a Nanodrop One C spectrophotometer (Labtech International) and quality
213 checked using an RNA Screen Tape on aTape Station instrument (Agilent Technologies). All the
214 extracted RNAs used in the subsequent analysis had an RNA integrity number (RIN^e) >6. Total RNA
215 (200ng) was labelled with Cy3-CTP using the Low input Quick Amp One Color labelling kit (Agilent
216 Technologies) and hybridized onto whole genome 8 X 60K mouse microarrays v2 (AMADID 074809)
217 following the manufacturer's instructions. The microarrays were washed and scanned using an
218 Agilent microarray scanner G2505C.

219 Transcriptome data analysis - Raw scanned microarray images were processed using Agilent Feature
220 Extraction software v11.5 and the data imported into R for normalization using the limma package
221 [33]. Microarray data were background corrected using the 'normexp' method (with an offset of 50),
222 quantile normalized and the data for technical replicates averaged. The processed data were then
223 filtered to remove probes exhibiting low signals across the arrays, retaining non-control probes that
224 are at least 10% brighter than negative control probe signals on at least three arrays. Data from
225 identical replicate probes was then averaged to produce expression values at the unique probe level.
226 Tests for differential expression were performed using the RankProd [34] package. Hierarchical
227 clustering was performed by complete linkage clustering and using the Pearson correlation for the
228 distance metric. Protein-protein interaction network construction and analysis, and functional
229 enrichment analysis at the protein level, was undertaken in Cytoscape [35] (v3.6.1; using the STRING
230 app (v1.4.0)[36] In STRING, confidence interaction scores of >0.4 or >0.7 were used to generate
231 medium and high confidence networks, respectively.

232 2. 16 Bioinformatic data mining

233 Kaplan-Meier survival curves for RFS and DMFS in breast cancer patients were generated using
234 KMplotter [37], (<http://kmplot.com/analysis/index.php?p=service>). The Cancer Genome Atlas
235 (TCGA) expression data according to breast cancer subtype was assessed and downloaded using
236 TCGA Portal (tumorsurvival.org).

237 2. 17 Other statistical analysis

238 Graphpad Prism v5.0 was used for the statistical analysis of all data other than the transcriptomics
239 data described above. For qPCR a one sample t-test was performed on using 1 as the hypothetical
240 value. For continuous data assuming normal variance a t-test or one-way analysis of variance was
241 used with Tukey's multiple comparisons tests between groups. Statistical significance was
242 determined where $p < 0.05$. All the results are representative of the mean of three or more
243 independent experiments ($n=3$) \pm SEM unless otherwise stated.

244 **2. 18 Data Availability**

245 The transcriptomics datasets are deposited in the ArrayExpress database at EMBL-EBI
246 (www.ebi.ac.uk/arrayexpress) under accession number E-MTAB-7299.

247 **3 Results**

248 3. 1 Glucocorticoids increase ROS/RNS production and DNA damage in murine breast cancer cells

249 Increases in NO production, have the potential to activate oncogenic pathways and induce genetic
250 instability through DNA damage [38]. The highly metastatic murine mammary carcinoma cell line
251 66CL4 was used as a model for aggressive triple negative breast cancer, and to validate previous
252 findings in human breast cancer cell lines [10]. To characterise the acute glucocorticoid exposure
253 ROS/RNS signature in 66CL4 cells; the cells were incubated with cortisol alongside the GR antagonist
254 RU486, as well as the non-specific NOS inhibitor N-Nitroarginine methyl ester (L-NAME) and
255 selective iNOS inhibitor 1400W dihydrochloride (1400W). Levels of intracellular nitrite, the stable by-
256 product of nitric oxide was measured using electrochemical sensors, and extracellular nitrite by the
257 Griess assay. Incubation with cortisol produced a significant increase in intracellular nitrite (Fig. 1A)
258 which was reversed with the addition of iNOS blockers L-NAME, 1400W and the GR antagonist,
259 RU486. Similarly, extracellular levels of nitrite were increased in response to cortisol and a significant
260 reduction was observed in response to RU486, 1400W and L-NAME, and this was validated using the
261 human breast cancer cell line MCF-7 (Fig. 1B). However, it should be noted that RU486 may also
262 inhibit progesterone receptors present on MCF-7 cells [39]. To confirm the effects of glucocorticoids
263 on nitrite production, the synthetic glucocorticoid dexamethasone (Dex) was also used to treat MCF-
264 7 cells. Dex increased levels of nitrite in a similar manner, however no significant difference was
265 observed between cortisol and dexamethasone treatment by either electrochemical detection or
266 Griess assay (Supplementary Figure 1A-B). 66CL4 cells were incubated with cortisol alongside GR
267 antagonist RU486 and cells were immunofluorescently stained for the GR. In response to cortisol,
268 translocation of the GR was observed and this was inhibited by RU486 (Supplementary Fig. 1C). The
269 expression of the GR mRNA remains unchanged in response to glucocorticoids (Supplementary Fig.
270 1D). To further explore the potential contribution of stress hormone signalling to tumour
271 invasiveness, 66CL4 cells were incubated with cortisol for 24hrs and the expression of iNOS, VEGF-A
272 and Twist1 was examined using qPCR. A significant increase in mRNA levels of iNOS was seen after
273 incubation in the presence of cortisol for 24hrs. A significant increase was also seen in expression of
274 VEGF-A and Twist1 after the addition of cortisol (Fig. 1C).

275 Previously glucocorticoids have been shown to induce DNA damage in human breast cancer cell
276 lines. To assess cortisol-induced damage a marker of DNA damage, phosphorylated γ -H2AX foci,
277 were visualised immunofluorescently in 66CL4 cells (Fig. 1D). In response to acute exposure to
278 cortisol the percentage of foci positive cells was significantly increased, and this effect was inhibited
279 by prior incubation with RU486 (Fig. 1E). RAD51 is involved in homologous recombination of double
280 stranded DNA breaks. Elevated levels of RAD51 correlate with poor clinical outcome in certain breast
281 cancers and RAD51 is often over expressed in human triple negative breast cancer cell lines [40].
282 RAD51 foci were examined in cells exposed to cortisol and a significant increase was observed,

283 which was reversed with the addition of RU486 (Fig. 1F). These *in vitro* analyses demonstrate that
284 murine mammary carcinoma cells respond to glucocorticoids in a similar manner to the human cell
285 lines previously examined [10].

286 To determine if the effect of cortisol on cell migration was mediated through increased expression of
287 iNOS, 66CL4 cells were transfected with siRNA directed towards *NOS2* (siNOS2) or a scrambled
288 control (siControl) (Fig. 1G). Cortisol significantly increased the migration of siControl transfected
289 66CL4 cells through transwell membranes, and knockdown of iNOS negated the effect of cortisol on
290 migration (Fig. 1H). Knockdown of *NOS2* also reduced the expression of the invasion-related genes
291 *TWIST1* and *VEGFA* (Supplementary Fig. 1E). Furthermore, using the *in vitro* scratch assay as a
292 measure of cell migration, treatment with cortisol was seen to promote migration, and this was
293 reduced by inhibition of the GR and iNOS (Supplementary Fig. 1G). To determine if cortisol or
294 inhibition of iNOS has effects on cell proliferation, 66cl4 cells were incubated with cortisol for 24
295 hours alongside RU486, as well as L-NAME. None of the treatments had an effect on cell
296 proliferation (Supplementary Fig. 1F). Taken together these results demonstrate that cortisol
297 increases the invasive potential of mammary tumour cells, through increased expression of
298 metastatic markers and NO signalling.

299 3.2 Inhibition of NOS reduces primary tumour growth and propensity for metastatic spread in 300 stressed mice

301 A syngeneic mouse model of highly metastatic mammary tumours was used to examine the effects
302 of psychological stress on tumourigenesis in combination with NOS inhibition. 66CL4 cells were
303 chosen as their route of dissemination has been characterised as rapidly colonizing the lung but not
304 liver, unlike 4T1 cells which colonise both [41]. Female mice bearing subcutaneous 66CL4 tumours
305 were randomized into groups and underwent a program of restraint stress (RS) – a model of
306 psychological stress known to induce sustained elevation of cortisol [42]. Groups were then further
307 stratified into saline (vehicle) treated or L-NAME, the pan-NOS inhibitor treated mice (Fig. 2A)

308 There was no significant difference in tumour volume observed after 14 days between vehicle and L-
309 NAME treated groups. In previous studies, reductions were seen after longer time courses as well as
310 in combination with conventional chemotherapies [14]. There was also no difference in primary
311 tumour volume between vehicle and stress groups, a normal observation in stress studies [43].
312 However, at 14 days a significant reduction in tumour volume was observed between the stress and
313 L-NAME + stress groups (Fig. 2B). The weight of the primary tumours was also reduced in L-NAME
314 treated groups, however not significantly so (Supplementary Fig. 2A). An increase in NO in the
315 tumour microenvironment can stimulate microvascularisation [44, 45], and it is therefore

316 hypothesised that inhibition of NOS may serve as a regulator of angiogenic activity. To evaluate the
317 degree of angiogenesis in the primary tumours, CD31 expression was immunofluorescently
318 quantified as a measure of microvessel density. There was no difference in microvessel density
319 between the vehicle and L-NAME treated groups. However, a significant increase in microvessel
320 density was observed in the stress group compared to the vehicle treated, and this was significantly
321 reduced in the L-NAME + stress group (Fig. 2C).

322 To examine the metastatic propensity of 66CL4 tumours in stressed mice, metastatic colonization of
323 the lung was examined using histopathology. Stressed mice had significantly more metastatic
324 nodules per lung compared to vehicle treated mice, and in stressed mice treated with L-NAME a
325 significant reduction in metastatic lung colonization was seen (Fig. 2D). The marker of proliferation
326 Ki67 was quantified in the metastases, and a significant increase was also seen in stressed mice
327 compared to vehicle treated (Fig. 2E). Twist1, a marker of metastasis which has been shown to
328 promote metastatic seeding and spread in breast cancer [46, 47], was quantified in the lungs of
329 experimental mice. The expression of Twist1 was significantly elevated in the lungs of stressed mice
330 compared to vehicle treated. Expression in stressed mice decreased with L-NAME treatment,
331 although still remained significantly higher than vehicle treated (Fig. 2F).

332 3.3 Stress differentially regulates genes associated with tumourigenesis in the lungs of tumour- 333 bearing mice

334 A transcriptomics analysis using microarrays was performed on the whole lungs of tumour-bearing
335 mice to probe the effects of stress on metastatic spread by identifying stress-related changes in gene
336 expression, and explore changes that can be reversed by L-NAME treatment (Fig. 3 and
337 Supplementary data 2). The results identified 212 genes that are significantly upregulated in the
338 stress group compared to the vehicle only control group, 18 of which are also significantly
339 downregulated in the L-NAME + stress cohort compared to the stress only group (Fig. 3A). Functional
340 analysis of the proteins encoded by the stress-induced transcripts indicates that stress provokes
341 changes in gene expression associated with cell division, proliferation and chemotaxis (Fig. 3B and
342 Supplementary data 2). Furthermore, of particular relevance were genes associated with cellular
343 response to DNA damage, blood vessel development and cell migration. Indeed, a significant
344 ($p < 1.0 \times 10^{-16}$) protein-protein interaction (PPI) network derived from the *Mus musculus* medium
345 confidence interactions curated in the STRING database [36] exhibits two connected sub-networks in
346 the stress-induced gene products, that are centred on a highly connected group of proteins required
347 for the mitotic cell cycle on the one hand, and cell chemotaxis and chemokine signalling on the other
348 (Fig. 3B). As expected from the data in Fig. 2F the Twist1 transcription factor is in the group of genes

349 identified as being significantly induced by stress, along with the related regulator Twist2.
350 Hierarchical clustering of the microarray transcript abundance data for the stress-induced genes was
351 used to identify groups of transcripts that are potentially co-regulated across the experimental
352 conditions and revealed a group of 75 containing all 18 of the stress-induced transcripts identified as
353 being responsive to correction by L-NAME (Fig. 3C). Analysis in STRING generated a significant PPI
354 network ($p = 1 \times 10^{-13}$) with components integral to the control of the mitotic cell cycle and
355 chemokine signalling, suggesting that L-NAME functions to ameliorate the effects of stress via
356 perturbations in these processes (Fig. 3C). The aurora kinase protein A (AURKA) is prominent as one
357 of the L-NAME reversible gene products identified in this analysis, and the network results suggest
358 an important role in the mediation of the effects of stress on breast cancer. AURKA is required for
359 correct progression through the mitotic cell cycle and has previously been implicated in
360 tumourigenesis, with increased expression associated with migration and metastasis [48-50]. It is
361 ca. 5-fold upregulated in the stressed mice, a change that is completely reversed by L-NAME
362 (Supplementary Fig. 2B), and, since it is also among the top 3% of most highly connected proteins in
363 the entire STRING mouse PPI network, this can be expected to generate extensive effects on cell
364 function. CCR2 chemokine receptor binding proteins are significantly enriched in the network in Fig.
365 3C, including CCL2, CCL7, CCL12. Increases in expression of the CCL2 gene, encoding a monocyte
366 chemoattractant, are associated with enhanced recruitment of infiltrating macrophages, promoting
367 metastasis and correlating with poor overall survival [51]. In addition, Arg1, a marker of M2
368 macrophages [52] was significantly upregulated in the lungs from stressed mice. Furthermore
369 S100/Ca-BP-9k-type calcium binding protein are also enriched. The S100A8 protein is secreted by
370 monocytes during the inflammatory response and is highly expressed in aggressive breast cancers
371 where it has been linked to the facilitation of invasion and metastasis [53, 54]. S100A8, S100A4 and
372 S100B are ligands for the Receptor for Advanced Glycation Endproducts (RAGE) and have been
373 implicated in RAGE-dependent signalling that plays diverse roles in cell biology and disease
374 processes, including inflammation, tumour outgrowth and metastatic colonisation [53-55].

375 Of the 36 genes that are significantly downregulated in the stressed mice compared to the control
376 group, only 2 are also significantly upregulated in the stress + L-NAME group compared to the stress
377 only cohort (Supplementary data 1). The proteins encoded by the stress-repressed gene are
378 significantly enriched for localization in the extracellular space (GO:0005615, $p=1.82E-08$) and for
379 functions associated with complement and coagulation cascades (KEGG 4610, $p=2.71E-05$) and
380 lipocalin binding (IPR002971, $p=7.56E-05$).

381 Genes that were identified as being induced by stress - but repressed by L-NAME in the metastatic
382 lungs of stressed mice - were also examined in relation to distant metastasis-free survival (DMFS) in

383 breast cancer patients (Fig. 3D). Patients were not stratified into subtype as the GR can be expressed
384 on both Luminal and HER2+ subtypes as well as basal. High expression of AURKA ($p=1.9e-8$, logrank
385 test) and S100A8 ($p=0.0012$, logrank test) were significantly correlated with poor probability of
386 DMFS. As was high expression of LMNB1 ($p=0.0013$, logrank test), which encodes for lamin B1 and
387 PRRX2 ($p=0.031$, logrank test), a transcription factor related to EMT.

388 3. 4 Stress associated genes are correlated with poor survival in invasive breast cancer subtypes

389 Glucocorticoids have been shown to regulate genes associated with breast cancer progression,
390 including genes involved in neoplasm invasiveness and cell transformation [7]. The clinical
391 importance of the glucocorticoid receptor (GR), as well as other genes linked to breast cancer
392 progression such as Twist1 - a transcription factor identified as essential for the metastatic process
393 [56] - was evaluated using survival analysis. The association between expression and recurrence-
394 free survival (RFS) was investigated using gene expression and survival data from a publicly available
395 microarray database (KM Plotter) [57]. Because we observed increases in NO_2^- in both TNBC and
396 luminal A cell lines, cohorts were stratified according to intrinsic subtype (Basal-like, HER2, Luminal
397 A, Luminal B) and further into high and low gene expression. Kaplan-Meier analysis shows high
398 expression of GR correlates with lower probability of RFS in basal-like breast cancer ($p=0.021$,
399 logrank test; Fig. 4A), but not in HER2 ($p=0.17$, logrank test; Fig. 1B), luminal A or B (Fig. 4C-D).
400 Similarly, high expression of Twist1 was shown to correlate with significantly worse probability of
401 RFS in basal-like ($p=0.0087$, logrank test; Fig. 4A) and HER2 ($p=0.028$, logrank test; Fig. 4B) breast
402 cancers, but not luminal A or B (Fig. 4C-D).

403 Increases in expression of iNOS in breast cancer have also been correlated with invasiveness and
404 increased vascularization [21], and aberrant NO signalling is linked to induction of angiogenesis
405 through stimulation of vascular endothelial growth factor (VEGF) [58, 59]. Mining of the publically
406 available TCGA breast cancer dataset was carried out in relation to iNOS (*NOS2*) and *VEGFA*, genes
407 closely involved in breast cancer progression. Expression of the chemokine *CCL2* similarly implicated
408 in breast cancer metastasis was also examined [60]. Comparison of the expression of *NOS2*, *VEGFA*
409 and *CCL2* across intrinsic subtypes of breast cancer demonstrates that these genes are significantly
410 associated with basal breast cancers compared to other subtypes (Fig. 4E-G).

411 3. 5 Cortisol promotes the release of pro-tumourigenic monocyte chemoattractants from breast 412 cancer-macrophage co-cultures

413 Glucocorticoids have been shown to activate tumour associated macrophages (TAM's), which play a
414 crucial role in tumour cell dissemination [61], as well as inducing polarization of macrophages to the

415 pro-tumourigenic M2 phenotype [62, 63], and upregulating anti-inflammatory mediators such as IL-
416 10 which also promote TAM recruitment and activation [64, 65]. In breast cancers the monocyte
417 chemoattractant C-C Motif Chemokine Ligand 2 (CCL2), produced by tumour cells to recruit and
418 polarize M2 macrophages, has been shown to correlate with decreased survival, as well an increase
419 in angiogenesis and metastasis [46, 51, 66].

420 In murine breast cancer cells (66CL4) treatment with cortisol significantly increased the expression
421 of CCL2 (Fig. 5A). In order to further investigate the role of glucocorticoids in potentially promoting
422 metastasis through an immune-mediated mechanism, 3D heterospheroids were cultured using
423 murine breast cancer cells and murine primary macrophages. Primary bone marrow-derived
424 monocytes (BMDM) were isolated, matured and polarized to either M1 or M2 macrophages.
425 Markers of polarization (M1 – iNOS, M2 – Arginase 1) were confirmed by qPCR (Fig. 5B-C).
426 Expression of the receptor for CCL2, CCR2 was also significantly increased in M2 macrophages, but
427 not M1, compared to an internal control (Fig. 5D). Macrophages were combined with 66CL4 cells
428 and grown as 3D heterospheroid co-cultures to model a tumour-TAM environment (Fig. 5E).
429 Spheroids were treated with cortisol and L-NAME alone and in combination for 7 days and levels of
430 CCL2 and IL-10 in the media were assayed. Cortisol treatment had no effect on levels of either CCL2
431 or IL-10 secreted by 66CL4+M1 spheroids. However levels of both CCL2 and IL-10 were significantly
432 increased in response to cortisol treatment of 66CL4+M2 spheroids. As expected, inhibition of NOS
433 using L-NAME had no effect alone, and in combination with cortisol did not affect the cortisol-
434 induced release of CCL2 or IL-10 (Fig. 5F-G).

435 **4 Discussion**

436 This study demonstrates the effects of glucocorticoids on pro-tumourigenic signalling and metastatic
437 spread in breast cancer, and identifies a novel role for NOS inhibition.

438 The results show that the stress hormone cortisol increases the production of RNS and DNA damage
439 through a NOS-mediated mechanism in mouse mammary tumour cells. A strong correlation has
440 been shown to exist between oxidative stress, DNA damage and tumourigenesis, however there has
441 been little conclusive evidence to suggest glucocorticoids exert a direct effect on this process.
442 Previous work has shown acute exposure to cortisol stimulates the production of RNS in human
443 breast cancer cell lines [10]. To confirm these effects would translate into an *in vivo* model of breast
444 cancer, a mouse mammary tumour line was studied. Cortisol was able to activate the GR in mouse
445 mammary tumour cells, and through GR activation increase levels of nitrite in a similar manner.
446 Pharmacological inhibition of NOS was able to reverse cortisol-mediated nitrite production, and
447 furthermore selective inhibition of iNOS proves that cortisol-induced generation of nitrite is

448 facilitated through iNOS specifically. In the same cell line, DNA damage and repair, as evidenced by
449 the formation of phosphorylated γ -H2AX foci and RAD51 foci, was also significantly increased in
450 response to cortisol. Inhibition of NOS was able to negate the effect of cortisol on DNA damage
451 indicating that the generation of NO is partly responsible for inducing DNA damage. Data from
452 microarray analysis also reveals that in the lungs of stressed mice pathways pertaining to response
453 to steroid hormone and response to DNA damage and were significantly enriched (Supplementary
454 data 1). Taken together these results demonstrate the involvement of cortisol-regulated NO in DNA
455 damage, and strengthens the hypothesis that one of the mechanisms through which exposure to
456 glucocorticoids may influence tumourigenesis is through the upregulation of oxidative stress.

457 Furthermore, the *in vitro* data also demonstrates that not only does cortisol upregulate expression
458 of iNOS, but also the expression of VEGF and Twist1, two pro-metastatic markers heavily involved in
459 the transformation to aggressive phenotypes. The deregulation of growth factor signalling is a
460 hallmark of tumourigenesis, and is usually observed in invasive tumours [67]. The production and
461 signalling of the potent angiogenic factor VEGF is often upregulated in the hypoxic tumour
462 microenvironment and plays a role in the increased NO signalling within tumours. VEGF binding
463 mobilizes intracellular calcium which induces eNOS and the production of NO, increasing the
464 angiogenic potential by creating a feedback mechanism whereby VEGF induces NO, and NO in turn
465 upregulates VEGF [58]. Therefore the increased NO signalling stimulated by glucocorticoids may
466 serve to promote angiogenesis through VEGF in a chronic stress model.

467 In our study, we found that cortisol can increase NO production in luminal A MCF-7 cells, however
468 although expression of GR correlated with lower probability of RFS in basal-like breast cancer it was
469 not significant in other breast cancer subtypes as previously described [8].

470 In the syngeneic mouse model of breast cancer used in this study, daily restraint stress - a well
471 characterised model of psychological stress - had no effect on primary tumour volume. This is in
472 keeping with previous studies, and supports the view that stress hormone signalling does not
473 directly affect primary tumour growth. The effects of chronic restraint stress on primary tumour
474 volume are instead much more pronounced when combined with chemotherapy, with stress
475 reducing the efficacy of chemotherapies in breast cancer [30], as well as in lung carcinoma [68].
476 Chronic stress alone has however been shown to affect the lymph vasculature surrounding the
477 primary tumour, with restraint stress significantly increasing the lymphatic network and metastasis
478 to the lymph node in a TNBC mouse model [5]. Similarly, in this study restraint stress significantly
479 increased the microvasculature of the primary tumour compared to the control, indicating that
480 whilst the tumours grew at the same rate, the primary tumours in stressed mice were more

481 aggressive and had an increased propensity for metastasis. Inhibition of NOS was able to exert a
482 significant effect on primary tumour growth when administered alongside restraint stress. There was
483 a significant reduction in primary tumour volume in the L-NAME + stress group compared to the
484 stress alone, as well as a reduction in microvasculature indicating an inhibition of angiogenic NO
485 signalling. As such the data gathered from this *in vivo* trial suggests that inhibition of NOS may be
486 able to reduce the pro-tumourigenic effect of psychological stress in breast cancer, through
487 reduction of NO-mediated angiogenesis. This is supported by the observation that stress significantly
488 increased metastatic colonization of the lungs and cell proliferation, both of which were reduced by
489 NOS inhibition.

490 However, whilst the inhibition of NOS alongside glucocorticoid treatment had effects on tumour
491 cells and *in vivo*, NOS inhibition had no effect on the cortisol-induced release of pro-tumourigenic
492 chemokines from breast cancer-macrophage spheroids. This may indicate a dual role for
493 glucocorticoids in metastatic processes, by which glucocorticoids promote the pro-inflammatory and
494 pro-tumourigenic release of NO from tumour cells, and the anti-inflammatory pro-metastatic
495 recruitment of M2 macrophages, which is an NO independent process (Fig. 6).

496 Twist1, a transcription factor known to promote EMT, invasiveness and metastasis, was upregulated
497 both *in vitro* in response to cortisol, and *in vivo* in the lungs of stressed mice. Furthermore,
498 interrogation of breast cancer data sets identified expression of both the GR and Twist1 as markers
499 of poor prognosis specifically in aggressive subtypes of breast cancer. This finding is consistent with a
500 previous discovery that activation of the GR is associated with poor prognosis in ER- breast cancers,
501 and is also linked to activation of epithelial-to-mesenchymal transition (EMT) pathways [8].
502 Increased NO signalling driven by an upregulation of iNOS expression in basal-like breast cancers can
503 also activate oncogenic signalling networks that induce EMT [69]. The data presented therefore
504 suggests a potential mechanism through which glucocorticoid signalling and can promote metastatic
505 dissemination and modulation of the tumour microenvironment through increased NO signalling
506 and upregulation of Twist1.

507 Interestingly, Twist1 has also been shown to modify the tumour microenvironment to promote
508 angiogenesis and metastasis by inducing the secretion of CCL2, and subsequently attracting
509 macrophages in a model of breast cancer [70]. Treatment with cortisol increased the expression of
510 CCL2 in 66CL4 cells alone, and in 66CL4-macrophage spheroids this result was verified, with levels of
511 CCL2 released significantly increasing as a result of cortisol treatment. It is unclear if in the
512 experiments presented here, cortisol induces the production of CCL2 directly, or as a result of
513 increased Twist1. However, the identification in the transcriptomics analysis of CCL2, as well as CCL7

514 and CCL12 as significantly induced in the lungs of stressed tumour-bearing mice provides further
515 indication that stress can promote metastasis through macrophage signalling. This finding is in
516 agreement with previous research detailing the role of β -adrenergic signalling on polarization of
517 macrophages to an M2-like phenotype [71]. Indeed the both arms of the stress response have well
518 characterised effects on immune function, with chronically elevated levels of glucocorticoids also
519 having been shown to be immunosuppressive [3]. Glucocorticoids have also been shown to
520 upregulate the expression of CCR2 - the receptor for CCL2, CCL7 and CCL12 - in human monocytes
521 [72], and enhance the migratory potential of monocytes through upregulation of CCR2 [73]. The M2
522 marker Arginase 1 (Arg1) was also identified as significantly upregulated by stress in the lungs,
523 suggesting that pro-tumourigenic M2 macrophages were being recruited as opposed to M1
524 macrophages [52, 74].

525 Similarly our transcriptome analysis also identified S100A8, another signalling protein involved in
526 macrophage-promoted tumour invasion, as being significantly induced by stress, an effect which was
527 then negated by NOS inhibition using L-NAME. At metastatic sites macrophages can induce
528 expression of S100A8, which enhances tumour cell migration and invasion, and acts as a marker of
529 tumour aggressiveness [53]. Although not explicitly related to immune cell function, the same
530 pattern of induction by stress and regulation by L-NAME was also observed with AURKA, which is
531 also heavily implicated in metastatic colonization in breast cancer [48, 75]. Furthermore
532 upregulation of paired-related homeobox1 (PRRX2), a transcription factor implicated in invasion and
533 the induction of EMT, is seen in response to stress and reduced upon treatment with L-NAME. The
534 stress-induced expression of these genes, and subsequent downregulation in stressed mice treated
535 with L-NAME, coupled with evidence that high expression is correlated with poor probability of
536 metastasis-free survival, indicates a mechanistic link between stress and metastasis in breast cancer.
537 Furthermore, the data suggests stress is able to modulate the function of M2-like macrophages and
538 alter cytokine signalling within the tumour microenvironment which promotes metastasis. This
539 cytokine signalling is not blocked by L-NAME, however it may represent another potential new
540 target for stress-mediated acceleration of cancer metastasis.

541 In conclusion, this study highlights new insights into the effect of stress hormone signalling on
542 tumorigenesis in a model of invasive breast cancer, and the potential therapeutic benefit of NOS
543 inhibition. This may be of relevance to highly stressed breast cancer patients, and especially to
544 patients with aggressive cancer subtypes such as basal, where an increase in the expression of the
545 GR and GR-mediated signalling may contribute to the spread of tumour cells.

546 **Author Contributions**

547 MSF participated in the design, conception, and coordination of studies and interpretation of the
 548 data and writing of the manuscript. RF prepared the manuscript, conducted the experiments and
 549 participated in the acquisition and interpretation of data. GB, AH and CPS participated in the design
 550 of the transcriptomics experiments. HI, MF, GB and AH assisted in the acquisition and interpretation
 551 of data and performed the statistical analysis. BAP designed, manufactured and characterised the
 552 sensors used. MCA and CPS contributed to data analysis. All authors read and approved the final
 553 manuscript.

554 **Acknowledgements**

555 The authors would like to thank Dr Erica Sloan for her contribution of cell lines, Myrthe Mampay for
 556 her assistance in BMDM isolation and Dr Graham Sheridan for critically reviewing the manuscript.
 557 Research was supported in part by the Boltini Trust.

558 **Conflicts of Interest**

559 The authors have no conflict of interest to disclose.

560 **References**

- 561 1. O'Connor, T.M., D.J. O'Halloran, and F. Shanahan, *The stress response and the hypothalamic-*
 562 *pituitary-adrenal axis: from molecule to melancholia*. Qjm-Monthly Journal of the
 563 Association of Physicians, 2000. **93**(6): p. 323-333.
- 564 2. Chida, Y., et al., *Do stress-related psychosocial factors contribute to cancer incidence and*
 565 *survival?* Nature Clinical Practice Oncology, 2008. **5**(8): p. 466-475.
- 566 3. Moreno-Smith, M., S.K. Lutgendorf, and A.K. Sood, *Impact of stress on cancer metastasis*.
 567 *Future Oncology*, 2010. **6**(12): p. 1863-1881.
- 568 4. Thaker, P.H., et al., *Chronic stress promotes tumor growth and angiogenesis in a mouse*
 569 *model of ovarian carcinoma*. Nature Medicine, 2006. **12**(8): p. 939-944.
- 570 5. Le, C.P., et al., *Chronic stress in mice remodels lymph vasculature to promote tumour cell*
 571 *dissemination*. Nature Communications, 2016. **7**.
- 572 6. Redig, A.J. and S.S. McAllister, *Breast cancer as a systemic disease: a view of metastasis*.
 573 *Journal of internal medicine*, 2013. **274**(2): p. 113-126.
- 574 7. Chen, Z., et al., *Ligand-dependent genomic function of glucocorticoid receptor in triple-*
 575 *negative breast cancer*. Nature communications, 2015. **6**: p. 8323.
- 576 8. Pan, D., M. Kocherginsky, and S.D. Conzen, *Activation of the Glucocorticoid Receptor Is*
 577 *Associated with Poor Prognosis in Estrogen Receptor-Negative Breast Cancer*. *Cancer*
 578 *Research*, 2011. **71**(20): p. 6360-6370.
- 579 9. Skor, M.N., et al., *Glucocorticoid receptor antagonism as a novel therapy for triple-negative*
 580 *breast cancer*. *Clinical cancer research : an official journal of the American Association for*
 581 *Cancer Research*, 2013. **19**(22): p. 10.1158/1078-0432.CCR-12-3826.
- 582 10. Flaherty, R.L., et al., *Glucocorticoids induce production of reactive oxygen species/reactive*
 583 *nitrogen species and DNA damage through an iNOS mediated pathway in breast cancer*.
 584 *Breast Cancer Research*, 2017. **19**.
- 585 11. Ranganathan, S., A. Krishnan, and N.D. Sivasithambaram, *Significance of twist and iNOS*
 586 *expression in human breast carcinoma*. *Molecular and Cellular Biochemistry*, 2016. **412**(1-2):
 587 p. 41-47.

- 588 12. Bentrari, F., et al., *Oct-2 forms a complex with Oct-1 on the iNOS promoter and represses*
589 *transcription by interfering with recruitment of RNA PolII by Oct-1*. *Nucleic Acids Res*, 2015.
590 **43**(20): p. 9757-65.
- 591 13. Glynn, S.A., et al., *Increased NOS2 predicts poor survival in estrogen receptor-negative breast*
592 *cancer patients*. *Journal of Clinical Investigation*, 2010. **120**(11): p. 3843-3854.
- 593 14. Granados-Principal, S., et al., *Inhibition of iNOS as a novel effective targeted therapy against*
594 *triple negative breast cancer*. *Breast cancer research : BCR*, 2015. **17**(1): p. 527.
- 595 15. Heinrich, T.A., et al., *Biological nitric oxide signalling: chemistry and terminology*. *British*
596 *Journal of Pharmacology*, 2013. **169**(7): p. 1417-1429.
- 597 16. Fukumura, D., S. Kashiwagi, and R.K. Jain, *The role of nitric oxide in tumour progression*.
598 *Nature Reviews Cancer*, 2006. **6**(7): p. 521-534.
- 599 17. Xu, W.M., et al., *The role of nitric oxide in cancer*. *Cell Research*, 2002. **12**(5-6): p. 311-320.
- 600 18. Nakamura, Y., et al., *Nitric oxide in breast cancer: Induction of vascular endothelial growth*
601 *factor-C and correlation with metastasis and poor prognosis*. *Clinical Cancer Research*, 2006.
602 **12**(4): p. 1201-1207.
- 603 19. De Paepe, B., et al., *Increased angiotensin II type-2 receptor density in hyperplasia, DCIS and*
604 *invasive carcinoma of the breast is paralleled with increased iNOS expression*. *Histochemistry*
605 *and Cell Biology*, 2002. **117**(1): p. 13-19.
- 606 20. Loibl, S., et al., *The role of early expression of inducible nitric oxide synthase in human breast*
607 *cancer*. *European Journal of Cancer*, 2005. **41**(2): p. 265-271.
- 608 21. Vakkala, M., et al., *Inducible nitric oxide synthase expression, apoptosis, and angiogenesis in*
609 *in situ and invasive breast carcinomas*. *Clin Cancer Res*, 2000. **6**(6): p. 2408-16.
- 610 22. Kostourou, V., et al., *The role of tumour-derived iNOS in tumour progression and*
611 *angiogenesis*. *British Journal of Cancer*, 2011. **104**(1): p. 83-90.
- 612 23. McCrudden, C.M., et al., *Systemic RALA/iNOS Nanoparticles: A Potent Gene Therapy for*
613 *Metastatic Breast Cancer Coupled as a Biomarker of Treatment*. *Molecular Therapy-Nucleic*
614 *Acids*, 2017. **6**: p. 249-258.
- 615 24. Vannini, F., K. Kashfi, and N. Nath, *The dual role of iNOS in cancer*. *Redox Biology*, 2015. **6**: p.
616 334-343.
- 617 25. Fitzpatrick, B., et al., *iNOS as a therapeutic target for treatment of human tumors*. *Nitric*
618 *Oxide*, 2008. **19**(2): p. 217-24.
- 619 26. Kisley, L.R., et al., *Genetic Ablation of Inducible Nitric Oxide Synthase Decreases Mouse Lung*
620 *Tumorigenesis*. *Cancer Research*, 2002. **62**(23): p. 6850.
- 621 27. Flint, M.S., et al., *Induction of DNA damage, alteration of DNA repair and transcriptional*
622 *activation by stress hormones*. *Psychoneuroendocrinology*, 2007. **32**(5): p. 470-479.
- 623 28. Li, Y., et al., *Electrochemical Detection of Nitric Oxide and Peroxynitrite Anion in*
624 *Microchannels at Highly Sensitive Platinum-Black Coated Electrodes. Application to ROS and*
625 *RNS Mixtures prior to Biological Investigations*. *Electrochimica Acta*, 2014. **144**: p. 111-118.
- 626 29. Fagan-Murphy, A., et al., *Electrochemical sensor for the detection of multiple reactive oxygen*
627 *and nitrogen species from ageing central nervous system homogenates*. *Mechanisms of*
628 *Ageing and Development*, 2016. **160**: p. 28-31.
- 629 30. Reeder, A., et al., *Stress hormones reduce the efficacy of paclitaxel in triple negative breast*
630 *cancer through induction of DNA damage*. *British journal of cancer*, 2015. **112**(9): p. 1461-70.
- 631 31. Ying, W., et al., *Investigation of macrophage polarization using bone marrow derived*
632 *macrophages*. *Journal of visualized experiments : JoVE*, 2013(76): p. 50323.
- 633 32. Tuominen, V.J., et al., *ImmunoRatio: a publicly available web application for quantitative*
634 *image analysis of estrogen receptor (ER), progesterone receptor (PR), and Ki-67*. *Breast*
635 *Cancer Research*, 2010. **12**(4): p. R56.
- 636 33. Ritchie, M.E., et al., *limma powers differential expression analyses for RNA-sequencing and*
637 *microarray studies*. *Nucleic Acids Res*, 2015. **43**(7): p. e47.

- 638 34. Breitling, R., et al., *Rank products: a simple, yet powerful, new method to detect differentially*
639 *regulated genes in replicated microarray experiments*. FEBS Lett, 2004. **573**(1-3): p. 83-92.
- 640 35. Shannon, P., et al., *Cytoscape: a software environment for integrated models of biomolecular*
641 *interaction networks*. Genome Res, 2003. **13**(11): p. 2498-504.
- 642 36. Szklarczyk, D., et al., *The STRING database in 2017: quality-controlled protein–protein*
643 *association networks, made broadly accessible*. Nucleic Acids Research, 2017. **45**(Database
644 issue): p. D362-D368.
- 645 37. Györfy, B., et al., *An online survival analysis tool to rapidly assess the effect of 22,277 genes*
646 *on breast cancer prognosis using microarray data of 1,809 patients*. Breast Cancer Res Treat,
647 2010. **123**(3): p. 725-31.
- 648 38. Ambs, S. and S.A. Glynn, *Candidate pathways linking inducible nitric oxide synthase to a*
649 *basal-like transcription pattern and tumor progression in human breast cancer*. Cell Cycle,
650 2011. **10**(4): p. 619-624.
- 651 39. Fazzari, A., et al., *The control of progesterone receptor expression in MCF-7 breast cancer*
652 *cells: effects of estradiol and sex hormone-binding globulin (SHBG)*. Mol Cell Endocrinol,
653 2001. **172**(1-2): p. 31-6.
- 654 40. Wiegman, A.P., et al., *Rad51 supports triple negative breast cancer metastasis*. Oncotarget,
655 2014. **5**(10): p. 3261-3272.
- 656 41. Aslakson, C.J. and F.R. Miller, *Selective Events in the Metastatic Process Defined by Analysis*
657 *of the Sequential Dissemination of Subpopulations of a Mouse Mammary Tumor*. Cancer
658 Research, 1992. **52**(6): p. 1399.
- 659 42. Gong, S., et al., *Dynamics and Correlation of Serum Cortisol and Corticosterone under*
660 *Different Physiological or Stressful Conditions in Mice*. PLoS ONE, 2015. **10**(2): p. e0117503.
- 661 43. Budiu, R.A., et al., *Restraint and Social Isolation Stressors Differentially Regulate Adaptive*
662 *Immunity and Tumor Angiogenesis in a Breast Cancer Mouse Model*. Cancer and clinical
663 oncology, 2017. **6**(1): p. 12-24.
- 664 44. Jadeski, L.C., et al., *Nitric oxide promotes murine mammary tumour growth and metastasis*
665 *by stimulating tumour cell migration, invasiveness and angiogenesis*. Int J Cancer, 2000.
666 **86**(1): p. 30-9.
- 667 45. Jadeski, L.C. and P.K. Lala, *Nitric Oxide Synthase Inhibition by N(G)-Nitro-L-Arginine Methyl*
668 *Ester Inhibits Tumor-Induced Angiogenesis in Mammary Tumors*. The American Journal of
669 Pathology, 1999. **155**(4): p. 1381-1390.
- 670 46. Qian, B.Z., et al., *CCL2 recruits inflammatory monocytes to facilitate breast-tumour*
671 *metastasis*. Nature, 2011. **475**(7355): p. 222-5.
- 672 47. Yang, J., et al., *Twist, a Master Regulator of Morphogenesis, Plays an Essential Role in Tumor*
673 *Metastasis*. Cell. **117**(7): p. 927-939.
- 674 48. Eterno, V., et al., *Aurka controls self-renewal of breast cancer-initiating cells promoting*
675 *wnt3a stabilization through suppression of miR-128*. Scientific Reports, 2016. **6**: p. 28436.
- 676 49. Siggelkow, W., et al., *Expression of aurora kinase A is associated with metastasis-free*
677 *survival in node-negative breast cancer patients*. BMC Cancer, 2012. **12**: p. 562.
- 678 50. Tang, A., et al., *Aurora kinases: novel therapy targets in cancers*. Oncotarget, 2017. **8**(14): p.
679 23937-23954.
- 680 51. Bonapace, L., et al., *Cessation of CCL2 inhibition accelerates breast cancer metastasis by*
681 *promoting angiogenesis*. Nature, 2014. **515**: p. 130.
- 682 52. Steggerda, S.M., et al., *Inhibition of arginase by CB-1158 blocks myeloid cell-mediated*
683 *immune suppression in the tumor microenvironment*. Journal for immunotherapy of cancer,
684 2017. **5**(1): p. 101-101.
- 685 53. Lim, S.Y., et al., *Tumor-infiltrating monocytes/macrophages promote tumor invasion and*
686 *migration by upregulating S100A8 and S100A9 expression in cancer cells*. Oncogene, 2016.
687 **35**: p. 5735.

- 688 54. Yin, C., et al., *RAGE-binding S100A8/A9 promotes the migration and invasion of human*
689 *breast cancer cells through actin polymerization and epithelial-mesenchymal transition.*
690 *Breast Cancer Res Treat*, 2013. **142**(2): p. 297-309.
- 691 55. Bresnick, A.R., D.J. Weber, and D.B. Zimmer, *S100 proteins in cancer.* *Nature reviews. Cancer*,
692 2015. **15**(2): p. 96-109.
- 693 56. Xu, Y., et al., *Twist1 promotes breast cancer invasion and metastasis by silencing Foxa1*
694 *expression.* *Oncogene*, 2017. **36**(8): p. 1157-1166.
- 695 57. Lanczky, A., et al., *miRpower: a web-tool to validate survival-associated miRNAs utilizing*
696 *expression data from 2178 breast cancer patients.* *Breast Cancer Res Treat*, 2016. **160**(3): p.
697 439-446.
- 698 58. Kimura, H. and H. Esumi, *Reciprocal regulation between nitric oxide and vascular endothelial*
699 *growth factor in angiogenesis.* *Acta Biochim Pol*, 2003. **50**(1): p. 49-59.
- 700 59. Konopka, T.E., et al., *Nitric Oxide Synthase II Gene Disruption - Implications for Tumor*
701 *Growth and Vascular Endothelial Growth Factor Production.* *Cancer Research*, 2001. **61**(7): p.
702 3182-3187.
- 703 60. Kitamura, T., et al., *CCL2-induced chemokine cascade promotes breast cancer metastasis by*
704 *enhancing retention of metastasis-associated macrophages.* *The Journal of Experimental*
705 *Medicine*, 2015. **212**(7): p. 1043.
- 706 61. Schmieder, A., et al., *Synergistic activation by p38MAPK and glucocorticoid signaling*
707 *mediates induction of M2-like tumor-associated macrophages expressing the novel CD20*
708 *homolog MS4A8A.* *Int J Cancer*, 2011. **129**(1): p. 122-32.
- 709 62. van de Garde, M.D., et al., *Chronic exposure to glucocorticoids shapes gene expression and*
710 *modulates innate and adaptive activation pathways in macrophages with distinct changes in*
711 *leukocyte attraction.* *J Immunol*, 2014. **192**(3): p. 1196-208.
- 712 63. Martinez, F.O. and S. Gordon, *The M1 and M2 paradigm of macrophage activation: time for*
713 *reassessment.* *F1000prime reports*, 2014. **6**: p. 13-13.
- 714 64. Ehrchen, J., et al., *Glucocorticoids induce differentiation of a specifically activated, anti-*
715 *inflammatory subtype of human monocytes.* *Blood*, 2007. **109**(3): p. 1265.
- 716 65. Williams, C.B., E.S. Yeh, and A.C. Soloff, *Tumor-associated macrophages: unwitting*
717 *accomplices in breast cancer malignancy.* *Npj Breast Cancer*, 2016. **2**: p. 15025.
- 718 66. Sierra-Filardi, E., et al., *CCL2 shapes macrophage polarization by GM-CSF and M-CSF:*
719 *identification of CCL2/CCR2-dependent gene expression profile.* *J Immunol*, 2014. **192**(8): p.
720 3858-67.
- 721 67. Hanahan, D. and R.A. Weinberg, *The hallmarks of cancer.* *Cell*, 2000. **100**(1): p. 57-70.
- 722 68. Zorzet, S., et al., *Restraint stress reduces the antitumor efficacy of cyclophosphamide in*
723 *tumor-bearing mice.* *Brain Behav Immun*, 1998. **12**(1): p. 23-33.
- 724 69. Switzer, C.H., et al., *S-Nitrosylation of EGFR and Src activates an oncogenic signaling network*
725 *in human basal-like breast cancer.* *Molecular cancer research : MCR*, 2012. **10**(9): p. 1203-
726 1215.
- 727 70. Low-Marchelli, J.M., et al., *Twist1 induces CCL2 and recruits macrophages to promote*
728 *angiogenesis.* *Cancer Res*, 2013. **73**(2): p. 662-71.
- 729 71. Lamkin, D.M., et al., *β -Adrenergic-stimulated macrophages: Comprehensive localization in*
730 *the M1-M2 spectrum.* *Brain, behavior, and immunity*, 2016. **57**: p. 338-346.
- 731 72. Yeager, M.P., et al., *Glucocorticoids enhance the in vivo migratory response of human*
732 *monocytes.* *Brain Behav Immun*, 2016. **54**: p. 86-94.
- 733 73. Yeager, M.P., et al., *Glucocorticoids enhance the in vivo migratory response of human*
734 *monocytes.* *Brain, behavior, and immunity*, 2016. **54**: p. 86-94.
- 735 74. Murray, P.J., et al., *Macrophage activation and polarization: nomenclature and experimental*
736 *guidelines.* *Immunity*, 2014. **41**(1): p. 14-20.

737 75. D'Assoro, A.B., et al., *The mitotic kinase Aurora--a promotes distant metastases by inducing*
 738 *epithelial-to-mesenchymal transition in ERalpha(+) breast cancer cells*. *Oncogene*, 2014.
 739 **33**(5): p. 599-610.

740

741

742

743

744

745

746

747 Figure Legends

748 **Fig. 1 Glucocorticoids increase ROS/RNS production and DNA damage in murine breast cancer**
 749 **cells. (A)** 66CL4 cells were incubated with cortisol +/- RU486, L-NAME and 1400W. Levels of
 750 intracellular nitrite (NO₂) were measured using electrochemical sensors. **(B)** 66CL4 and MCF-7 cells
 751 were incubated with cortisol +/- RU486 and L-NAME. Extracellular nitrite levels were quantified
 752 using the Griess assay. **(C)** 66CL4 cells were incubated with cortisol for 24hrs and the expression of
 753 *NOS2*, *VEGFA*, *TWIST1* and *ACTB* quantified using qPCR. Ct values were normalised against β -actin
 754 and fold change calculated using the delta-Ct method. **(D)** Cells were immunofluorescently stained
 755 for phosphorylated γ -H2AX and RAD51. Representative images shown. **(E-F)** Cells with >5 foci were
 756 scored as positive and expressed as % of total cells. **(G)** 66CL4 cells were transfected with *NOS2*-
 757 directed siRNA (siNOS2) or scrambled control siRNA (siControl) and expression of iNOS quantified by
 758 western blot. **(H)** siControl or siNOS2 transfected 66CL4 cells were plated onto transwell permeable
 759 supports and treated with cortisol for 4 hours. Migrated tumour cells were stained and counted.
 760 Data expressed as number of cells/field. Mean \pm SEM expressed and statistical significance was
 761 determined one sample t-test, one way or two way ANOVA (post hoc Tukey's multiple comparisons).
 762 * = $p < 0.05$, ** = $p < 0.01$, *** = $p < 0.001$.

763 **Fig. 2 Inhibition of NOS reduces primary tumour growth and propensity for metastatic spread in**
 764 **stressed mice. (A)** 66CL4 mouse mammary tumour cells were transplanted into the fourth mammary
 765 fat pad of female BALB/C mice. Groups were exposed to restraint stress (2hrs/day)(n=8) or no stress
 766 (Vehicle)(n=9), in combination with L-NAME treatment (80mg/kg)(n=7). **(B)** Primary tumour volume.
 767 Data presented as mean +/- SEM. **(C)** (Right) Primary tumours were immunofluorescently stained for
 768 CD31 expression, representative panels shown, (left) microvessel density was quantified and
 769 expressed as mean +/- SEM. **(D)** Lungs were resected and sections taken midway through the lung
 770 were stained with H&E to quantify metastatic nodules. (Right) Arrows indicate metastatic nodules,
 771 representative panels shown, scale = 1mm. **(E)** Lung sections were immunohistochemically stained
 772 for Ki67, and staining intensity quantified using ImmunoRatio. (Right) representative images shown.
 773 **(F)** RNA was extracted from a whole resected lung and the expression of *TWIST1* and *ACTB*
 774 quantified using qPCR. Ct values were normalised against β -actin and relative expression calculated
 775 using the delta-Ct method. Mean \pm SEM expressed, for box-plots whiskers: min to max. Statistical
 776 significance was determined using one or two way ANOVA (post hoc Tukey's multiple comparisons).
 777 * = $p < 0.05$, ** = $p < 0.01$, *** = $p < 0.001$.

778 **Fig. 3 Stress differentially regulates genes associated with tumorigenesis in the lungs of tumour-**
 779 **bearing mice.** Transcriptomics analysis identifies changes in gene expression in the whole lungs of
 780 tumour-bearing mice subjected to combinations of confinement stress (Stress) and treatment with
 781 the NOS inhibitor L-NAME. (A) Numbers of significantly differentially expressed transcripts identified
 782 between the treatment groups using Rank Products analysis (Vehicle control group, n=4; Stress, n=3;
 783 L-NAME, n=3; Stress + L-NAME, n=3). Analysis of the overlap between the treatment groups
 784 identifies significant stress-related changes in transcription that are reversible by L-NAME treatment.
 785 Full details are provided in Supplementary data 1. (B) The 223 transcripts significantly upregulated in
 786 the lungs of stressed tumour bearing mice compared to the vehicle control group are enriched for
 787 functions associated with cell proliferation, chemotaxis and blood vessel development (see
 788 Supplementary data 1 for the complete analysis). A protein-protein interaction network derived
 789 from the *Mus musculus* medium confidence (0.4) interaction network in the STRING database shows
 790 two connected sub-networks in the stress-induced gene products. Only connected nodes are shown:
 791 the network for all nodes is significantly enriched for interactions compared to randomized sets, p-
 792 value $< 1 \times 10^{-16}$ (C). Stress-induced transcripts that co-cluster with the 19 L-NAME responsive stress-
 793 induced transcripts generate a significant PPI network ($p = 1 \times 10^{-13}$) which suggests roles for Aurka,
 794 Ccl2 and certain S100 proteins (see also Supplementary data 1). (D) High/low expression of *AURKA*,
 795 *S100A8*, *LMNB1* and *PRRX2* and distant metastasis-free survival (DMFS) was compared.

796 **Fig. 4 Stress associated genes are correlated with poor survival in invasive breast cancer subtypes.**
 797 Breast cancer microarray datasets were stratified into subtype; (A) Basal-like, (B) HER2, (C) Luminal
 798 A and (D) Luminal B, and further into high/low expression of NR3C1 (GR) or TWIST1, recurrence-free
 799 survival (RFS) was compared using Kaplan-Meier survival plots. Expression of (E) NOS2, (F) VEGFA
 800 and (G) CCL2 was examined in the TCGA data set of breast cancers (n=908). Comparison of
 801 expression levels in intrinsic subtypes was carried out using one-way ANOVA and Tukey's multiple
 802 comparison test. Mean \pm SEM expressed, for box-plots whiskers: 5-95 percentiles. Statistical
 803 significance was determined using one way ANOVA (post hoc Tukey's multiple comparisons). * =
 804 $p < 0.05$, ** = $p < 0.01$, *** = $p < 0.001$.

805 **Fig. 5 Cortisol promotes the release of pro-tumourigenic monocyte chemoattractants from breast**
 806 **cancer-macrophage co-cultures.** (A) 66CL4 cells were incubated with cortisol for 24hrs and the
 807 expression of *CCL2* and *ACTB* quantified using qPCR. (B-D) Bone marrow-derived macrophages
 808 (BMDM) were isolated, matured and polarized to M1 or M2. Markers of polarization (*NOS2*, *ARG-1*)
 809 and *CCR2* were quantified using qPCR. Ct values were normalised against β -actin and relative
 810 expression vs an internal reference calculated using the delta-Ct method. (E) Macrophages were co-
 811 cultured with 66CL4 breast cancer cells to form 3D spheroids, and incubated with cortisol +/- L-
 812 NAME for 7 days. Representative images shown. (F) Media from the spheroid co-cultures was
 813 removed and assayed for CCL2 and IL-10 using ELISA. Levels were normalized to protein extracted
 814 from spheroids. Mean \pm SEM expressed and statistical significance was determined using students t-
 815 test or two way ANOVA (post hoc Tukey's multiple comparisons). * = $p < 0.05$, ** = $p < 0.01$, *** =
 816 $p < 0.001$.

817 **Fig. 6. Glucocorticoids promote metastatic dissemination through increased NO-mediated DNA**
 818 **damage and angiogenic signalling, as well as through immunomodulation.**

819 **Supplementary Fig. 1(A)** MCF-7 cells were incubated with cortisol or dexamethasone (Dex). Levels of
 820 intracellular nitrite (NO_2) were measured using electrochemical sensors. (B) Extracellular nitrite
 821 levels were quantified using the Griess assay. (C) Cells were stained for the glucocorticoid receptor
 822 (GR) (green) and counterstained with DAPI (blue). (D) 66CL4 cells were treated with cortisol for
 823 30mins or 24hrs. Expression of the glucocorticoid receptor (*NR3C1*) was quantified using qPCR. Ct

824 values were normalised against β -actin and fold change calculated using the delta-Ct method. **(E)**
825 66CL4 cells were transfected with *NOS2*-directed siRNA (siNOS2) or scrambled control siRNA
826 (siControl) the expression of *NOS2*, *VEGFA*, *TWIST1* and *ACTB* quantified using qPCR. Ct values were
827 normalised against β -actin and fold change calculated using the delta-Ct method. **(F)** 66CL4 cells
828 were incubated with cortisol +/- RU486, L-NAME and 1400W and cell viability measured using the
829 MTT assay. Viability expressed at a percentage of control. **(G)** 66CL4 cells were grown to confluency
830 and a wound made in the monolayer. Area closure indicates migration and is expressed as are
831 closure normalised to area at 0hrs.

832 **Supplementary Fig. 2 (A)** 66CL4 mouse mammary tumour cells were transplanted into the fourth
833 mammary fat pad of female BALB/C mice. Groups were exposed to restraint stress (2hrs/day) or no
834 stress (Vehicle), in combination with L-NAME treatment (80mg/kg). Primary tumours were weighed
835 at necropsy **(B)** Transcript abundance of *AURKA* in the resected lungs of experimental mice
836 quantified by microarray expression analysis.

837

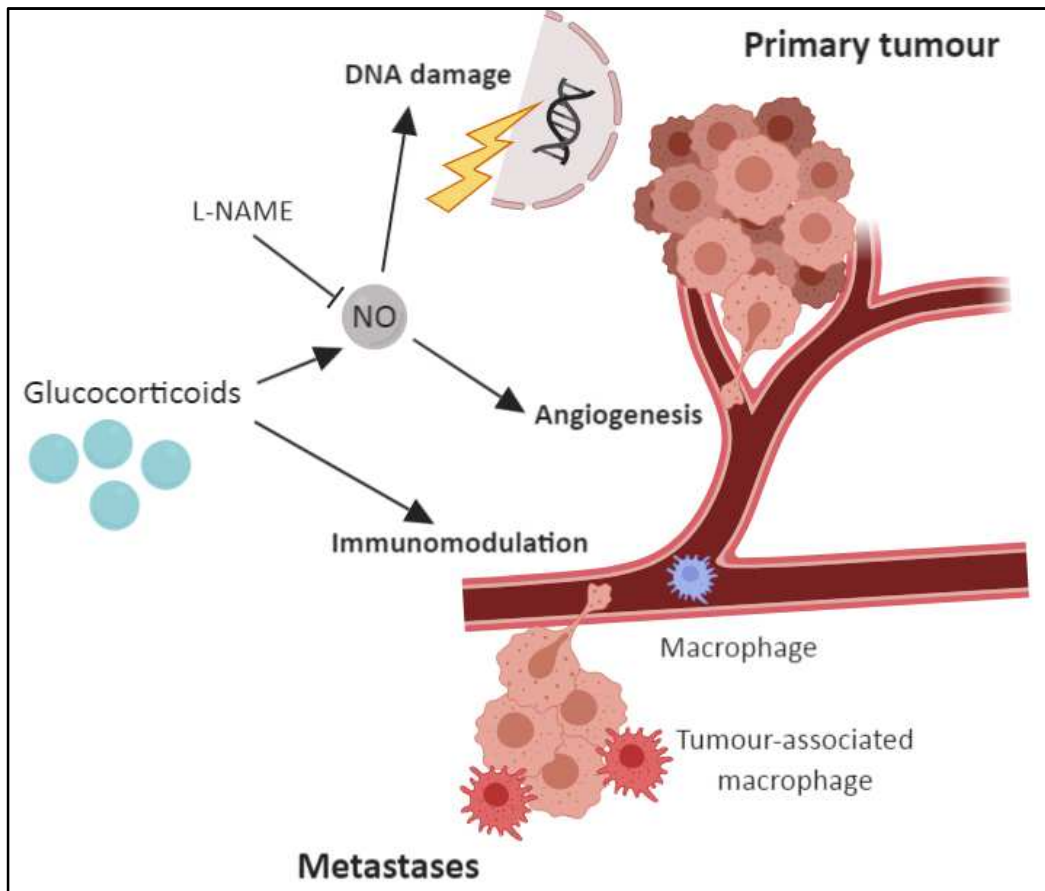
838

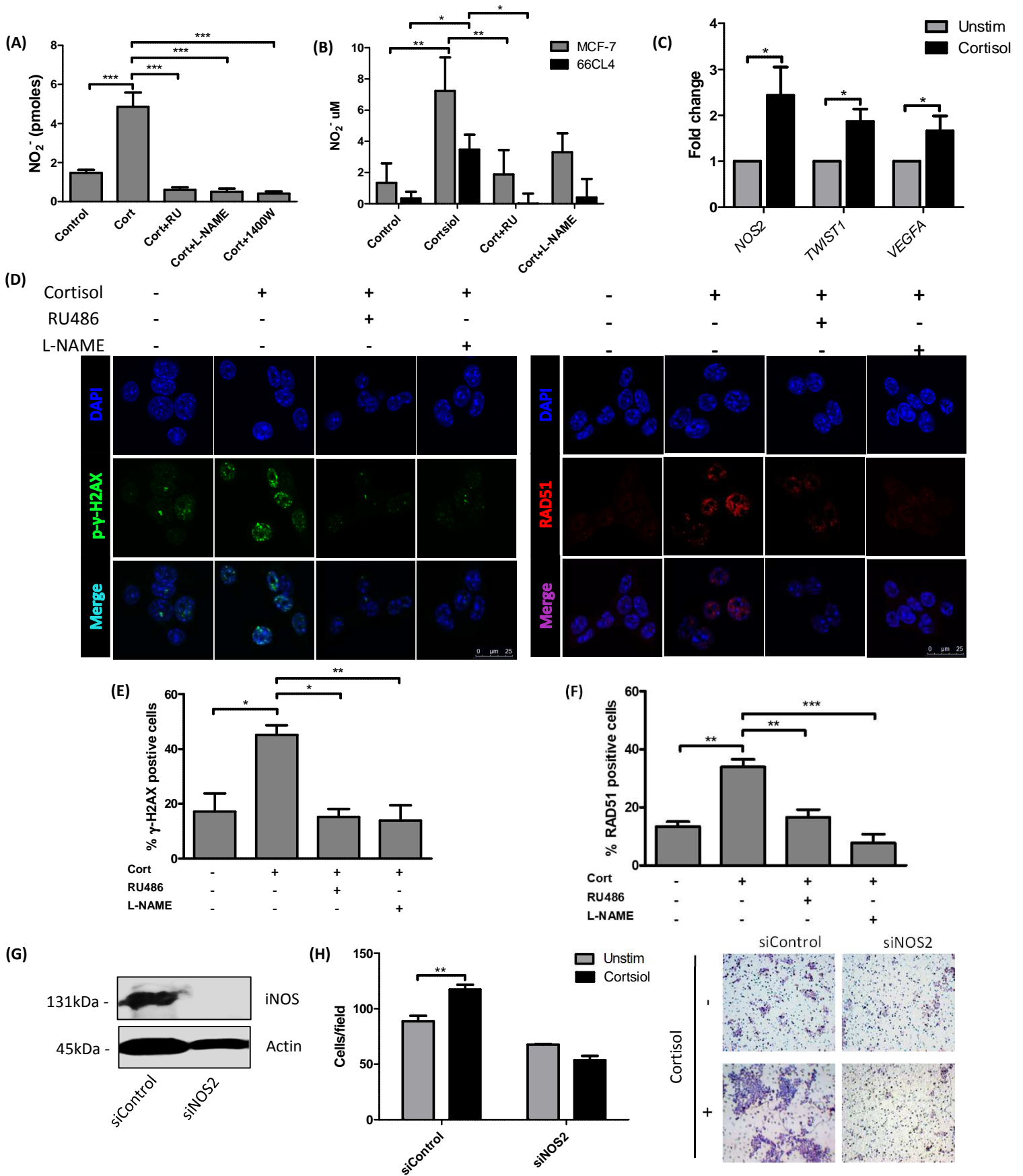
839

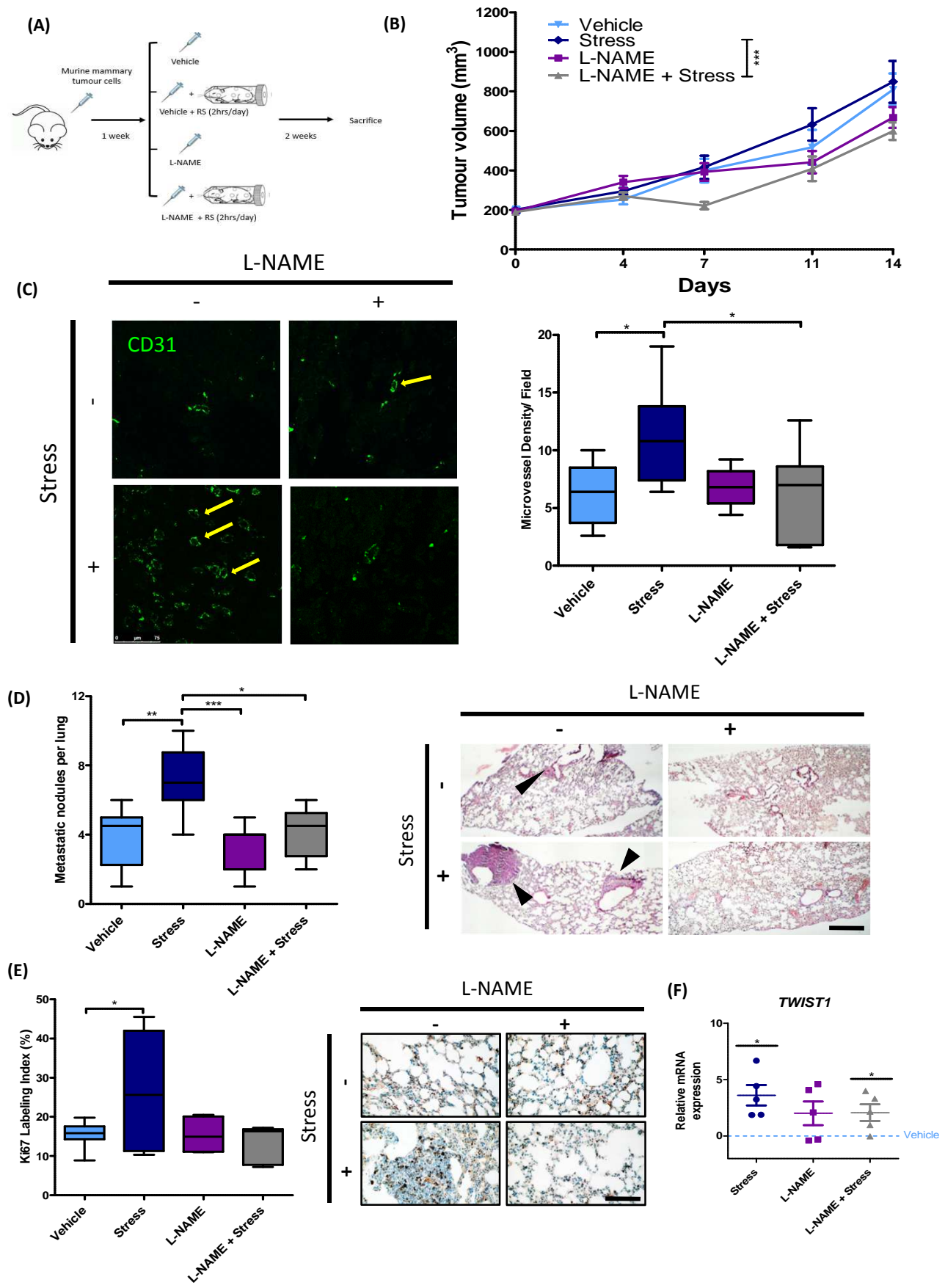
840

841

Figure 6







(A)

	Numbers of sig. genes (pfp<=0.1)	
	Down	Up
Vehicle vs Stress	36	212
Vehicle vs L-NAME	0	0
Stress vs L-NAME + Stress	177	62
L-NAME vs L-NAME + Stress	0	0

(B)

(B) Protein-protein interaction network for gene products significantly induced by stress

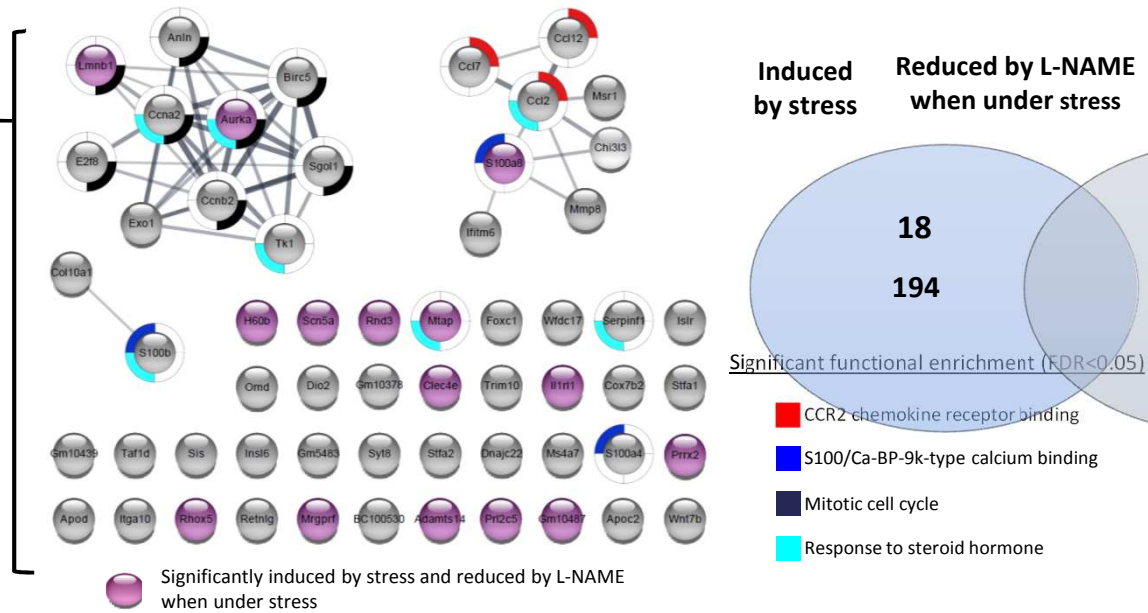
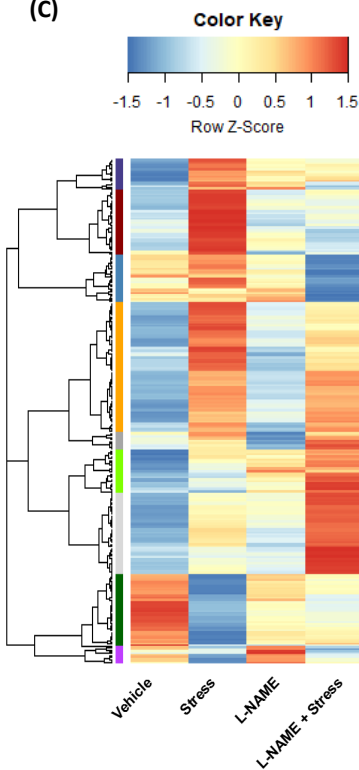
55 proteins, enriched for:

Pathway Description	Gene Count	FDR
Cell cycle (GO:0007049)	37	3.91E-34
Microtubule cytoskeleton (GO:0015630)	31	2.49E-07
Cellular response to stress (GO:0033554)	13	9.49E-04
p53 signalling pathway (KEGG 4115)	4	1.32E-03

22 proteins, enriched for:

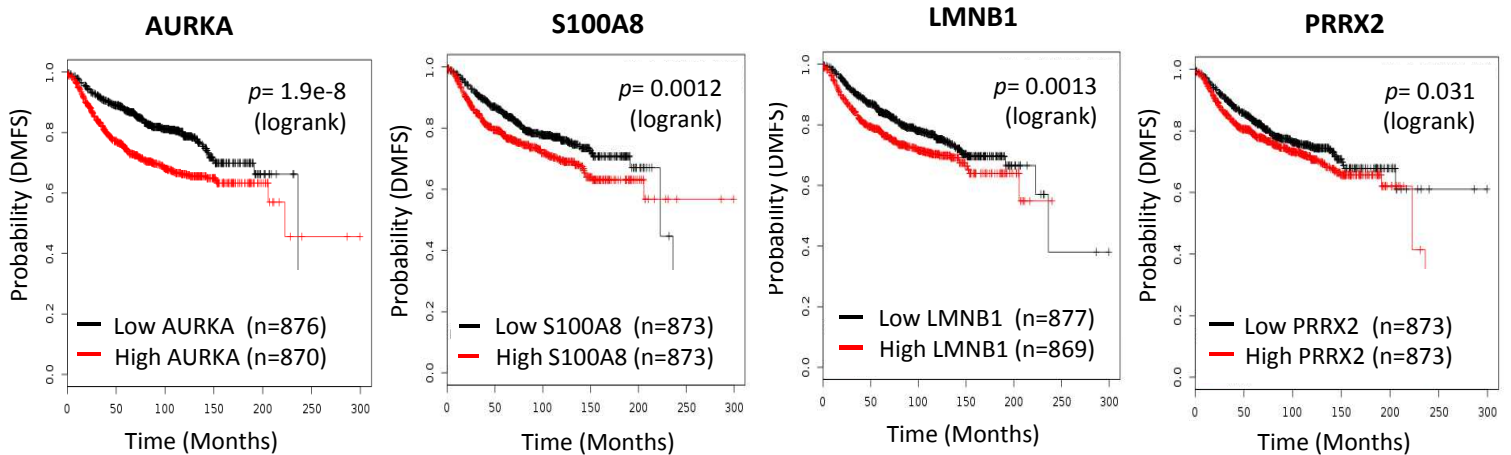
Pathway Description	Gene Count	FDR
Cell chemotaxis (GO:0060326)	8	5.84E-09
Chemokine signalling pathway (KEGG 4062)	4	8.05E-03
Response to oxygen-containing compound (GO:1901700)	7	1.11E-02
Blood vessel development (GO:0001568)	5	1.15E-02

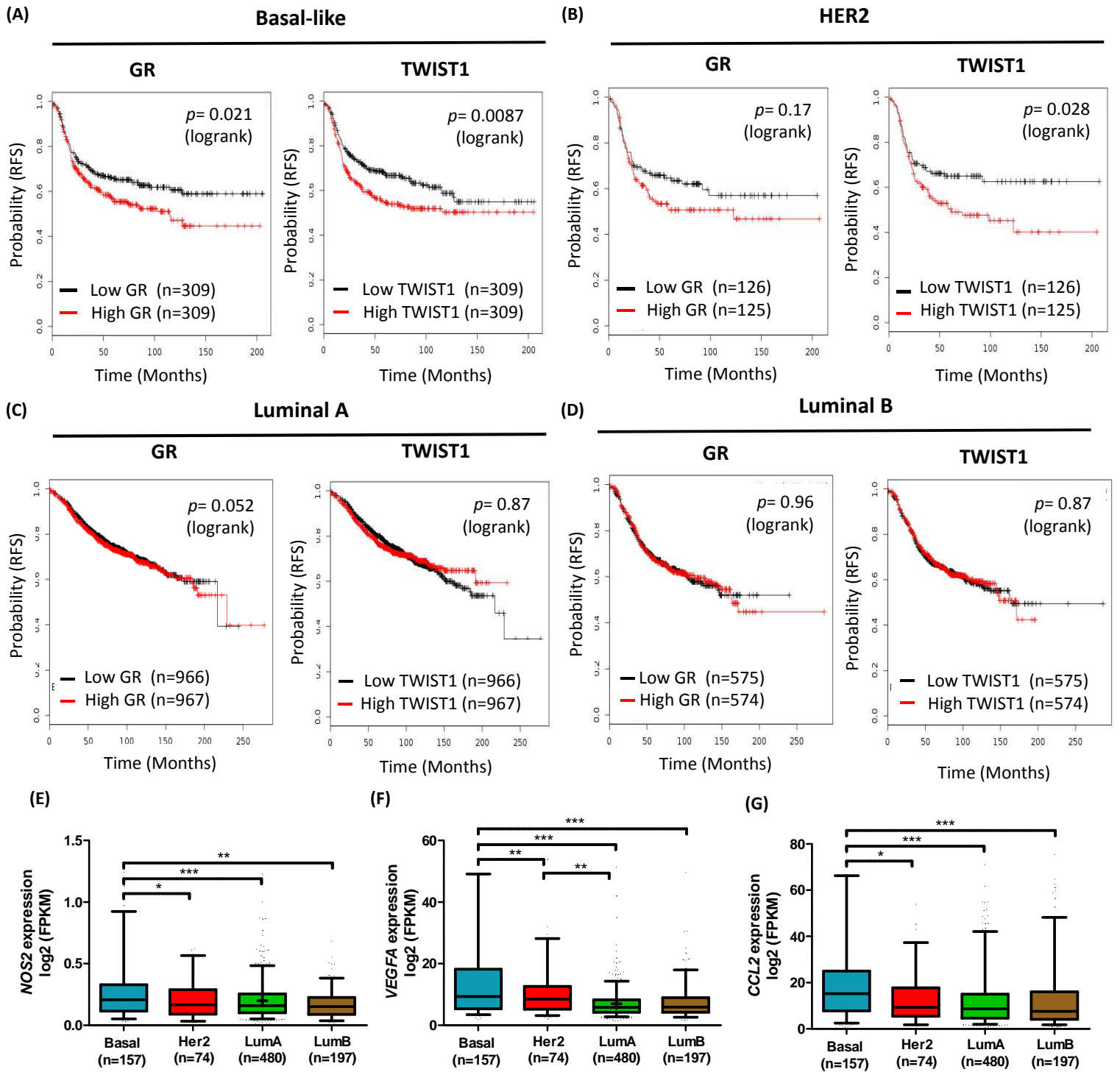
(C)

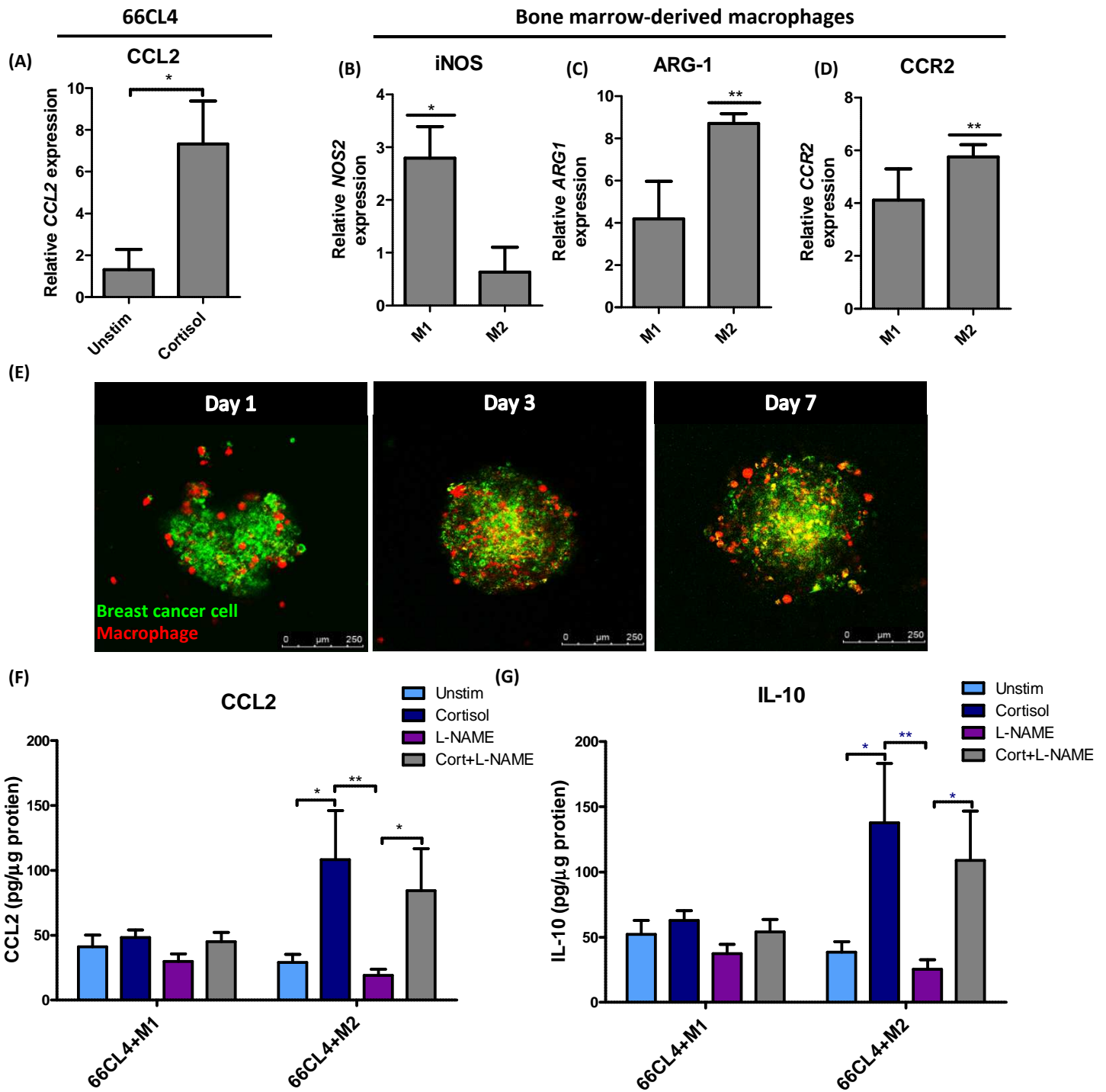


(D)

Genes induced by stress and repressed by L-NAME







Highlights

- The stress hormone cortisol increases production of reactive nitrogen species (RNS) and induces DNA damage through a nitric oxide synthase (NOS)-mediated mechanism in breast cancer cells
- Psychological stress promotes metastatic spread, and this is reversed by inhibition of NOS *in vivo*.
- Stress induces expression of genes associated with tumorigenesis in the lungs of tumour bearing-mice.
- Cortisol promotes the release of pro-tumorigenic monocyte chemoattractants from breast cancer-macrophage co-cultures

Conflicts of Interest

The authors have no conflict of interest to disclose.

ACCEPTED MANUSCRIPT